



## Cyclodextrin-derived polymer networks for selective molecular adsorption†

Cite this: *Chem. Commun.*, 2020, 56, 11783

Received 15th July 2020,  
Accepted 7th September 2020

DOI: 10.1039/d0cc04784h

rsc.li/chemcomm

Bailey Phillips,<sup>a</sup> Chenxu Wang,<sup>b</sup> Xinman Tu,<sup>b</sup> Che-Hsuan Chang,<sup>a</sup> Sarbajit Banerjee,<sup>ab</sup> Mohammed Al-Hashimi,<sup>d</sup> Wei Hu<sup>e</sup> and Lei Fang<sup>\*ab</sup>

**A facile synthetic method is developed to afford cyclodextrin-derived polymer networks that exhibit high selectivity in capturing certain organic compounds in water. The sustainable and scalable synthesis, together with the highly robust adsorption performance enables efficient removal and/or separation of organic molecules from aqueous solution in a continuous flow system.**

Selective molecular adsorption is critical to sensing, separation, environmental remediation, and many other applications.<sup>1,2</sup> During adsorption of small organic molecules, selectivity is often achieved by either specific non-covalent interactions or size-matching between the adsorbent backbone and the adsorbate molecules.<sup>3,4</sup> Besides selectivity, practical applications often demand the adsorbent materials to be robust in the operational conditions, easy to use and recycle, and inexpensive to produce.<sup>5</sup> Many porous materials, such as covalent organic frameworks, conjugated microporous polymers, and hyper-crosslinked polymers,<sup>6</sup> have been extensively investigated for this purpose. Among these, bottom-up synthesized, crosslinked porous polymer networks are an intriguing class of adsorbents due to their versatile structural tunability, facile synthesis, and resistance to dissolution.<sup>7,8</sup> Macrocyclic molecules such as calixarenes,<sup>9,10</sup> pillararenes,<sup>11,12</sup> cyclodextrins,<sup>11,13,14</sup> and crown ethers,<sup>15,16</sup> have been incorporated into porous polymer networks, with the promise of combining the advantages of

supramolecular hosts and porous polymer networks for selective molecular adsorption. These materials have indeed exhibited unprecedented efficiency and selectivity that was not accessible on conventional adsorbent materials, such as activated carbon.<sup>17</sup>

Despite exciting recent advancements achieved in supramolecular host-incorporated adsorbent polymers, it is still challenging to deploy them in large scale applications partially due to the need for inexpensive, efficient, and environmentally friendly synthesis of these materials. From a perspective of macrocyclic starting materials, cyclodextrins are ideal because they can be produced in a sustainable, low cost manner.<sup>18,19</sup> Cyclodextrins are composed of glucopyranosidic repeating units that possess rich hydroxyl functional groups on the outer side of the macrocycle, enabling potential self-condensation reactions for crosslinking.<sup>20</sup> Once crosslinked into a solid network, the juxtaposition of the hydrophobic cavity and hydrophilic outer side of the macrocycle yields a hydrophilic polymer network that can selectively capture hydrophobic guest molecules inside the cyclodextrin cavity.<sup>20</sup> Herein, by taking full advantage of these features of cyclodextrin, we report an extraordinarily facile and scalable synthesis of linker-less cyclodextrin-derived polymer networks (CD-PNs), and their excellent selectivity towards adsorbing organic molecules in aqueous media. This approach affords robust materials, while being highly sustainable and scalable for future industrial application.

In this work, a methanesulfonic acid (MSA)-mediated condensation reaction was developed to crosslink  $\beta$ - or  $\alpha$ -cyclodextrin monomers, to afford the polymer networks  $\beta$ -CD-PN and  $\alpha$ -CD-PN, respectively (Fig. 1). During the synthesis, cyclodextrin monomers were dissolved in MSA and heated at 110 °C for ~48 h without any protection from water or oxygen, followed by simple washing as the work up. In this acid-promoted reaction, the hydroxyl groups on glucopyranoside units from different cyclodextrin monomers undergo ether condensation to crosslink them into a polymer network. The formation of the ether linkages is supported by the emergence of a strong C–O–C stretching peak at 1157 cm<sup>-1</sup> in the FTIR spectra of CD-PNs (Fig. S4 and Table S2, ESI†).<sup>21</sup>

<sup>a</sup> Department of Chemistry, Texas A&M University, College Station, Texas 77843, USA. E-mail: fang@chem.tamu.edu

<sup>b</sup> Department of Materials Science and Engineering, Texas A&M University, College Station, Texas 77843, USA

<sup>c</sup> Key Laboratory of Jiangxi Province for Persistent Pollutants Control and Resources Recycle, College of Environmental and Chemical Engineering, Nanchang Hangkong University, Nanchang 330063, China. E-mail: tuxinman@126.com

<sup>d</sup> Department of Chemistry, Texas A&M University at Qatar, P. O. Box 23874, Doha, Qatar

<sup>e</sup> Department of Electronic Engineering, Tsinghua University, Beijing 100084, China. E-mail: weihu@mail.tsinghua.edu.cn

† Electronic supplementary information (ESI) available: Synthetic methods, characterization data, procedures for adsorption tests. See DOI: 10.1039/d0cc04784h

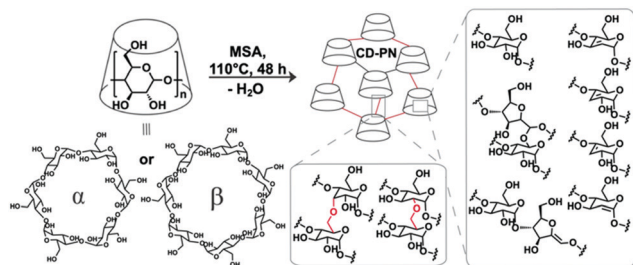


Fig. 1 Synthetic scheme and proposed reaction scheme of CD-PN.

At the optimized temperature of 110 °C, the water byproduct is driven out of the solution to push forward the ether condensation *via* thermodynamic control yielding a fully crosslinked, insoluble product. Other than the dehydrative ether condensation, dehydrative  $\beta$ -elimination also takes place during the reaction, affording  $sp^2$ -carbons in the product as evidenced by XPS and solid-state NMR (Fig. S2 and S3, ESI<sup>†</sup>). However, excessive  $\beta$ -elimination is avoided at the optimized temperature of 110 °C in order to prevent the formation of an overly hydrophobic material that would not be favorable for aqueous applications. The extent of dehydration, associated with both ether condensation and  $\beta$ -elimination, was estimated based on the isolated yields and elemental analysis data. Taking  $\beta$ -CD-PN as an example, the isolated yield is calculated to be 64% based on the mass of the monomer, corresponding to  $\sim 22.69$  mol of water loss per mol of  $\beta$ -cyclodextrin. On the other hand, by comparing the elemental composition of  $\beta$ -CD-PN (found: C, 66.50; H, 4.70; O, 28.00; S, <0.05%) with the starting material,  $\beta$ -cyclodextrin (found: C, 44.45; H, 6.22; O, 49.30%), one can estimate  $\sim 19.46$  mol of water loss per mol of  $\beta$ -cyclodextrin in the reaction. These values agree well with each other despite the small error in the measurement of yield and elemental analysis. It is worth noting that other strong acid-promoted side-reactions, such as isomerization of the glucopyranosidic

building block into a glucofuranoside structure through ring opening and re-annulation, are also possible (Fig. 1).<sup>22</sup>

The simple MSA-promoted reaction carries a number of advantages for practical adsorption applications. First, despite the undefined chemo- and regio-selectivity of the reaction, the important macrocyclic constitution of the cyclodextrin unit was expected to be preserved during the crosslinking, so that the resulting CD-PNs inherit the capability of selective guest adsorption from cyclodextrin. Second, this reaction takes advantage of using inexpensive and non-toxic MSA as the catalyst and solvent simultaneously, without the addition of any other reagent, ensuring the sustainability and scalability of the synthesis.<sup>23,24</sup> Thirdly, the pristine nature of this reaction, involving only solvent and monomer, allows for versatile and amenable solution processing of the material through *in situ* crosslinking<sup>25</sup> into a desired form and morphology, such as well-defined smooth thin films that maintain the structure and performance of the bulk material (Fig. S5, S7, S9 and S13, ESI<sup>†</sup>). Last but not least, the cyclodextrin monomer is crosslinked directly with no additional spacer affording the CD-PNs with the theoretical potential for a maximized density of macrocyclic binding sites.

$N_2$  adsorption isotherm of  $\beta$ -CD-PN showed low measurable surface area ( $<10$   $m^2$   $g^{-1}$ ). Despite this lack of apparent porosity, the presence of macrocyclic binding sites with defined sizes promises CD-PNs to be good selective adsorbent materials for small molecules dissolved in water, as has been noted for other cyclodextrin-based polymers. The adsorption selectivity and capacitance were investigated using model aqueous solutions of small molecular dyes (Fig. 2b). The sizes of the dye molecules were estimated to better understand the adsorption potential of both  $\alpha$ - and  $\beta$ -CD-PN (Fig. S11, ESI<sup>†</sup>). The CD-PN materials were first ground into powders and subsequently added to the tested dye solution while stirring with UV-vis absorbance spectroscopy being recorded to determine the



Fig. 2 (a) Schematic representation and digital photograph of column separation using  $\beta$ -CD-PN as the adsorbent (flow rate  $\sim 0.4$   $mL$   $s^{-1}$ ); (b) structures of tested small molecular dyes; column dye adsorption data of (c)  $\beta$ -CD-PN (d)  $\alpha$ -CD-PN (e) Glu-PN and (f) activated carbon ( $C$  = eluent concentration,  $C_0$  = feed concentration). In Fig. 2f, all dye adsorption data are overlapping except for Congo red.

adsorption efficiency. As expected, organic molecules that are smaller than the  $\beta$ -cyclodextrin cavity, such as bisphenol A (BPA) and methylene blue, are efficiently adsorbed by  $\beta$ -CD-PN with fast adsorption kinetics (Fig. S12, ESI<sup>†</sup>), while larger dye molecules, such as rose Bengal, rhodamine B, and Congo red, are not adsorbed. In contrast, no significant adsorption of the dye molecules was observed for  $\alpha$ -CD-PN owing to its smaller cavity size. Although  $\beta$ -CD-PN displayed fast adsorption properties, it is important to note that the kinetics are limited by diffusion, morphology, and particle size, so these measurements may not be completely representative of an intrinsic chemical property of the material. Nevertheless, Langmuir adsorption isotherms of  $\beta$ -CD-PN exhibited remarkably high adsorption capacities for methylene blue and BPA (177.8 and 387.9 mg g<sup>-1</sup>, respectively, see Fig. S14 and S15, ESI<sup>†</sup>). The BPA adsorption capacity surpasses those reported on most other cyclodextrin-derived polymer networks (Table S3, ESI<sup>†</sup>), supporting the hypothesis that the linker-less  $\beta$ -CD-PN has the potential to reach a maximized density of binding sites compared to those requiring a crosslinker during synthesis.

These adsorption results, in conjunction with the scalability of the synthesis, suggest that  $\beta$ -CD-PN can be employed as a filler adsorbent for energy-efficient separation of organic molecules in aqueous solution. Model flow-through separation experiments were conducted in a miniature column using a 1 mL syringe (Fig. 2a). The model column contained approximately 100 mg of adsorbent. An aqueous feed solution containing a molecular dye or a mixture of dyes was continuously fed through the column with a flow rate of  $\sim 0.4$  mL s<sup>-1</sup>, while the eluent was collected in fractions for analysis. As expected,  $\beta$ -CD-PN exhibits highly efficient adsorption with exemplary selectivity for BPA and methylene blue (Fig. 2c). For BPA, 99% adsorption efficiency was maintained for the full duration of the 60 mL feed solution (0.2 mM). While for methylene blue 99% adsorption efficiency was maintained for the first 32 mL of feed solution with over 90% adsorption efficiency continuing up to 53 mL of feed solution (0.2 mM). On the other hand,  $\alpha$ -CD-PN had minimal adsorption for molecules of all sizes due to its small cavity size (Fig. 2d). Only BPA and rose Bengal exhibit marginal adsorption. The BPA adsorption can be attributed to hydrogen bonding interactions with BPA by the residual hydroxyl groups on  $\alpha$ -CD-PN. The small amount of adsorption of large rose Bengal molecule is likely due to the partial inclusion of the iodide group into the  $\alpha$ -cyclodextrin cavity.<sup>26</sup> This result indicates that careful selection of the macrocycle based on cavity size is critical for achieving different levels of selectivity, which can be extended to various adsorbates.

To further confirm the important role of macrocyclic binding sites in engendering selective adsorption, the performance of two control materials, namely, commercial activated carbon and a crosslinked network of glucose (**Glu-PN**) without the presence of cyclodextrin-like macrocycles, were investigated and compared. **Glu-PN** was synthesized under the same MSA-mediated conditions using D-(+)-glucose as the starting material. Flow-through adsorption tests on **Glu-PN** showed almost no uptake of all tested molecules. Only a small uptake

of BPA (Fig. 2e) was observed likely due to hydrogen bonding, agreeing with that observed on  $\alpha$ -CD-PN. In contrast, commercial activated carbon exhibited vast adsorption uptake of all tested organic molecules without any selectivity (Fig. 2f) as a result of the rich presence of pores with a broad size distribution. These adsorption data demonstrate that the macrocyclic backbone in  $\beta$ -CD-PN is essential for the observed adsorption selectivity and also suggests that the macrocyclic cavity is retained from the cyclodextrin monomers throughout the synthesis despite the strong conditions.

The extent of selective adsorption performance of  $\beta$ -CD-PN was further confirmed by the adsorption of small organic molecules in the presence of a high concentration of interfering non-adsorbing organic molecules. In this study, the adsorption of methylene blue (0.005 mM) was tested in the presence of an excess amount of rhodamine B (0.1 mM) (methylene blue : rhodamine B = 1 : 20).  $\beta$ -CD-PN exhibited complete adsorption of methylene blue while adsorbing little to no rhodamine B (Fig. 3a). In comparison,  $\alpha$ -CD-PN adsorbed a small amount of methylene blue and very little rhodamine B (Fig. 3b). **Glu-PN** adsorbed a minimal amount of rhodamine B and no methylene blue (Fig. 3c). Activated carbon, in contrast, displayed no selectivity by completely adsorbing both dyes (Fig. 3d). These data further demonstrate the excellent size selectivity of the  $\beta$ -CD-PN, while also showing its strong affinity for molecules with size and shape complementarity even amongst a substantial amount of interference. It is important, however, to note that while selectivity is retained, the adsorption capacity is somewhat impacted potentially due to intermolecular interactions between the dye molecules.<sup>27</sup> Additionally, it is expected that the adsorption properties can be enhanced with careful morphological control, which can be achieved through *in situ* crosslinking enabled by the pristine nature of the MSA mediated reaction.

The crosslinked nature of  $\beta$ -CD-PN not only renders it suitable for column separation applications while mitigating

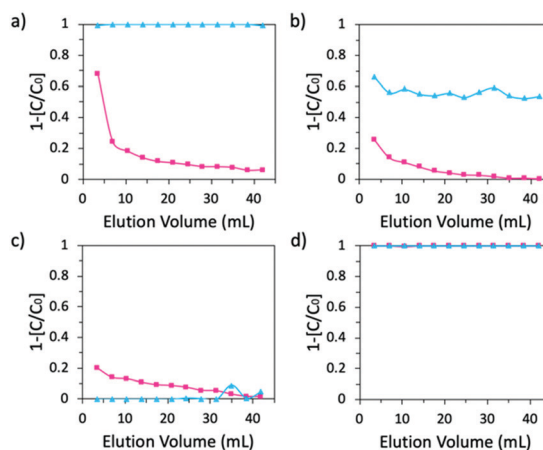


Fig. 3 Adsorption performance of a mixture of 0.005 mM methylene blue + 0.1 mM rhodamine B by (a)  $\beta$ -CD-PN (b)  $\alpha$ -CD-PN (c) **Glu-PN** and (d) activated carbon. In Fig. 3d, the data points for methylene blue and rhodamine B are overlapping.

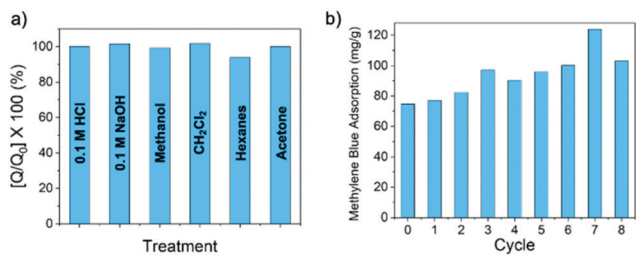


Fig. 4 (a) Adsorption performance of  $\beta$ -CD-PN to methylene blue after variable chemical treatments ( $Q$  = adsorption after treatment,  $Q_0$  = base-line adsorption). (b) Recyclability of  $\beta$ -CD-PN methylene blue adsorption where cycle 0 is the first use.

concerns related to sloughing and dissolution, but also imparts an enhanced robustness into the polymer network that is not inherent in the cyclodextrin monomers. It showed remarkable chemical resistance with little to no loss in methylene blue adsorption performance after exposure to strong aqueous acid or base, or strong organic solvents (Fig. 4a).  $\beta$ -CD-PN also exhibited exemplary recyclability after regeneration by simply washing with methanol from a saturated adsorbed state. In fact, the adsorption performance was not only maintained but also slightly improved after being regenerated from washing (Fig. 4b), presumably due to a decreased particle size after washing and wearing that rendered the binding sites more accessible to the adsorbate. The simple washing regeneration procedure for  $\beta$ -CD-PN is a low energy process furthering its industrial practicality, especially compared with activated carbons, which typically require very high energy regeneration processes.<sup>28,29</sup>

In conclusion, the sustainable and scalable synthesis of dehydrated cyclodextrin-derived polymer networks was achieved *via* a facile MSA-mediated condensation reaction. The retained macrocyclic cavities in  $\beta$ -CD-PN enable its exceptional selective adsorption on organic small molecules that match the cyclodextrin cavity size, such as BPA and methylene blue, even in the presence of a highly concentrated interfering compound. To put this result in context,  $\beta$ -CD-PN was compared with other cyclodextrin-derived polymers in terms of BPA adsorption capacities and synthetic conditions (Table S3, ESI<sup>†</sup>), demonstrating its high adsorption performance as a result of the linker-less synthetic strategy along with enhanced synthetic sustainability and scalability. Moreover, the crosslinked network imparts a high level of robustness into the materials with both thermal and chemical stability, as well as cyclability through a low energy-consuming regeneration process. The combined advantages of this class of CD-PNs promise their future application in fine chemicals/pharmaceutical separation, sensing, and environmental remediation. Furthermore, it is expected that with careful morphological control, which is enabled by the simplistic synthesis, the CD-PNs present a powerful platform for advancing both fundamental knowledge and applications of cyclodextrin-based materials.

The authors acknowledge support for this work by the Qatar National Priority Research Program (NPRP10-0111-170152), the Robert A. Welch Foundation (A-1898), the Natural Science Foundation of Jiangxi Province (20192ACBL20042) and National Natural Science Foundation of China (U1731117). W. H. thanks the support by a Chinese Academy of Sciences Scholarship. Use of TAMU Materials Characterization Facility is acknowledged.

## Conflicts of interest

There are no conflicts to declare.

## Notes and references

- 1 B. Phillips, S. Banerjee, X. Tu and L. Fang, *Supramol. Chem.*, 2020, **32**, 165–177.
- 2 J. Murray, K. Kim, T. Ogoshi, W. Yao and B. C. Gibb, *Chem. Soc. Rev.*, 2017, **46**, 2479–2496.
- 3 J. M. Lehn, *Angew. Chem., Int. Ed. Engl.*, 1988, **27**, 89–112.
- 4 X. F. Ji, R. T. Wu, L. L. Long, C. X. Guo, N. M. Khashab, F. H. Huang and J. L. Sessler, *J. Am. Chem. Soc.*, 2018, **140**, 2777–2780.
- 5 P. A. Julien, C. Mottillo and T. Friscic, *Green Chem.*, 2017, **19**, 2729–2747.
- 6 S. Das, P. Heasman, T. Ben and S. L. Qiu, *Chem. Rev.*, 2017, **117**, 1515–1563.
- 7 Z. H. Guo, C. X. Wang, Q. Zhang, S. Che, H. C. Zhou and L. Fang, *Mater. Chem. Front.*, 2018, **2**, 396–401.
- 8 J. Huang and S. R. Turner, *Polym. Rev.*, 2018, **58**, 1–41.
- 9 D. Shetty, J. Jahovic, J. Raya, Z. Asfari, J. C. Olsen and A. Trabolsi, *ACS Appl. Mater. Interfaces*, 2018, **10**, 2976–2981.
- 10 C. Heath, B. Pejic and M. Myers, *New J. Chem.*, 2017, **41**, 6195–6202.
- 11 P. P. Lu, J. C. Cheng, Y. F. Li, L. Li, Q. Wang and C. Y. He, *Carbohydr. Polym.*, 2019, **216**, 149–156.
- 12 B. B. Shi, H. X. Guan, L. Q. Shangguan, H. Wang, D. Y. Xia, X. Q. Kong and F. H. Huang, *J. Mater. Chem. A*, 2017, **5**, 24217–24222.
- 13 A. Alsaiee, B. J. Smith, L. L. Xiao, Y. H. Ling, D. E. Helbling and W. R. Dichtel, *Nature*, 2016, **529**, 190–U146.
- 14 Z. H. Wang, F. C. Cui, Y. W. Pan, L. X. Hou, B. Zhang, Y. Q. Li and L. P. Zhu, *Carbohydr. Polym.*, 2019, **213**, 352–360.
- 15 Q. W. Li, W. Y. Zhang, O. S. Miljanic, C. H. Sue, Y. L. Zhao, L. H. Liu, C. B. Knobler, J. F. Stoddart and O. M. Yaghi, *Science*, 2009, **325**, 855–859.
- 16 T. Xu, Y. He, Y. Qin, C. X. Zhao, C. J. Peng, J. Hu and H. L. Liu, *RSC Adv.*, 2018, **8**, 4963–4968.
- 17 Y. H. Ling, M. J. Klemes, L. L. Xiao, A. Alsaiee, W. R. Dichtel and D. E. Helbling, *Environ. Sci. Technol.*, 2017, **51**, 7590–7598.
- 18 A. Biwer, G. Antranikian and E. Heinzle, *Appl. Microbiol. Biotechnol.*, 2002, **59**, 609–617.
- 19 J. Szejtli, *Pure Appl. Chem.*, 2004, **76**, 1825–1845.
- 20 E. V. Anslyn and D. A. Dougherty, *Modern physical organic chemistry*, University Science, Sausalito, CA, 2006.
- 21 S. T. Feng, C. Bagia and G. Mpourmpakis, *J. Phys. Chem. A*, 2013, **117**, 5211–5219.
- 22 S. J. Dee and A. T. Bell, *ChemSusChem*, 2011, **4**, 1166–1173.
- 23 T. Palden, B. Onghena, M. Regadio and K. Binnemans, *Green Chem.*, 2019, **21**, 5394–5404.
- 24 Y. Zou, T. Y. Yuan, H. Q. Yao, D. J. Frazier, D. J. Stanton, H. J. Sue and L. Fang, *Org. Lett.*, 2015, **17**, 3146–3149.
- 25 C. Wang, C. Li, E. R. C. Rutledge, S. Che, J. Lee, A. J. Kalin, C. Zhang, H.-C. Zhou, Z.-H. Guo and L. Fang, *J. Mater. Chem. A*, 2020, **8**, 15891–15899.
- 26 J. Haller and U. Kaatze, *J. Mol. Liq.*, 2008, **138**, 34–39.
- 27 D. D. Do and H. D. Do, *Appl. Surf. Sci.*, 2002, **196**, 13–29.
- 28 I. Ali, M. Asim and T. A. Khan, *J. Environ. Manage.*, 2012, **113**, 170–183.
- 29 E. Menya, P. W. Olupot, H. Storz, M. Lubwama and Y. Kiros, *Chem. Eng. Res. Des.*, 2018, **129**, 271–296.